Journal of Applied Mechanics and Technical Physics, Vol. 39, No. 1, 1998

THREE-DIMENSIONAL TOMOGRAPHY IN GAS FLOW DIAGNOSTICS IN THE PRESENCE OF AN OPAQUE BODY

A. V. Likhachev and V. V. Pikalov

UDC 533.9+518.517.948+533.605

The possibility of tomographic reconstruction of the density distribution in a three-dimensional gas flow with a complex structure is considered. The effect of the presence of an opaque body on the reconstruction results is studied. Specific features of the inverse problem that are associated with practical realization of the experiment, namely, a small number of viewing angles and the presence of noise in projection data, are taken into account in numerical simulation.

Tomographic methods have been widely used in physical experiments in recent decades. The main area of application of tomography is the diagnostics of a low- or high-temperature plasma (see, for example, [1–3]). However, the present-day level of technology and engineering allows one to apply tomography in many other applications. Some problems dealing with the use of tomographic methods in gas dynamics were considered in [4, 5]. Vukičević et al. [6] reconstructed very accurately the temperature field in the cross section of a convective flow of heated air on the basis of variations in its refractive index. Data obtained by the method of holographic interferometry were processed using tomographic algorithms.

From the viewpoint of tomography, Vukičević et al. [6] reconstructed a function of two variables using a set of its one-dimensional projections. The present paper presents the reconstruction of a function of three variables that describes the three-dimensional distribution of the refractive index in a flow, from its two-dimensional projections. This problem will be called below a problem of three-dimensional tomography. Some aspects of three-dimensional tomography were considered in [4, 7]. Despite great informativeness, three-dimensional tomography is seldom used in physical experiments because of technical difficulties in the collection of projection data, on the one hand, and the large amount of computations, which increases in an attempt to achieve better spatial resolution, on the other hand.

The present paper is devoted to problems that can arise in an experiment on three-dimensional tomographic reconstruction of a flow density. Since the object of study in gas dynamics is often a flow around a solid body, which is usually optically opaque, we consider the effect of the presence of an opaque body in a flow on the reconstruction results. The specific features of the problem of three-dimensional tomography with high spatial resolution are also studied. Some aspects of this problem were considered in [8]. Special attention is paid to problems connected with the small number of viewing angles, their nonuniform distribution over the angles, and the presence of noise in projection data.

1. Formulation of the Problem. Two formulations of the problem of three-dimensional tomography are considered.

(1) Let there be no opaque body. The problem can be formulated as follows. The function $g(x, y, z)$ is reconstructed inside a bounded domain $\Omega \subset \mathrm{R}^3$ from a finite set of its projections $f_m(u, v)$, $m = 1, \ldots, M$ (3 is one of the projections in Fig. 1). The function $f(u, v)$ in Fig. 1 is defined on a plane D that does not cross Ω. The value of $f(u, v)$ at some point of the plane D is the integral of $g(x, y, z)$ along the straight line that passes through this point and is perpendicular to the plane D.

Institute of Theoretical and Applied Mechanics, Siberian Division, Russian Academy of Sciences, Novosibirsk 630090. Translated from Prikladnaya Mekhanika i Tekhnicheskaya Fizika, Vol. 39, No. 1, pp. 174–180, January–February, 1998. Original article submitted May 6, 1996.

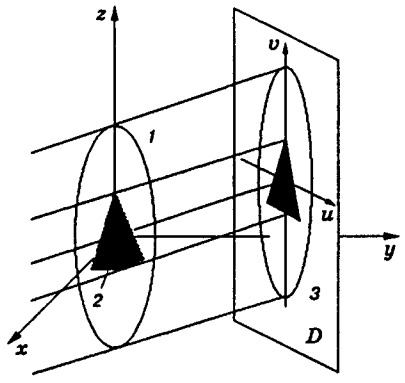

Fig. 1

(2) Let there be an opaque body 2. In this case, the above problem is complicated. We again reconstruct the function $g(x,y,z)$ from the set of functions $f_m(u,v)$, where $m = 1,\ldots,M$. Nevertheless, now the values of $f_m(u,v)$ are not everywhere equal to the integrals of $g(x,y,z)$ along the straight lines. The projection has a zero value in the region shaded by the opaque body. This shadow is shown in Fig. 1 as a black triangle in the plane D. Thus, the presence of an opaque body leads to loss of part of the information on the gasdynamic object 1 being examined.

Projection data for the problem of three-dimensional tomography can be obtained, for example, by the methods of holographic interferometry. In this case, the functions $f_m(u,v)$ describe the phase difference when the corresponding beam passes through the domain Ω in the presence or absence of the examined disturbance of the medium. This quantity can be related to the total (along the beam) variation in the refractive index. Thus, the function $g(x,y,z)$ is equal to the difference of the refractive indices of the medium and the object. Having reconstructed the function $g(x,y,z)$ by tomographic methods and knowing the refractive index of the medium, we can determine the refractive index of the object. Holographic interferometry is described in detail in [5], and its use to obtain tomographic data can be found in [6].

2. The Algorithms Used. The problem of three-dimensional tomography described in Sec. 1 was preliminarily discretized in the usual way by Herman [7]. The reconstruction domain was sampled into cubic voxels, and the value of the function $g(x,y,z)$ in each voxel was assumed to be constant. Square grids were defined on the support of each projection, and each node in these grids was correlated with one beam along which the integration was performed. The value of $f_m(u,v)$ at a node was equated to the integral along this beam. After discretization, the problem of three-dimensional tomography reduces to the system of linear algebraic equations

$$Ag = f. \tag{2.1}$$

Here A is a matrix of dimensions $I \times J$, $g \in \mathrm{R}^J$, $f \in \mathrm{R}^I$, and g and f are vectors corresponding to the reconstructed function and the projection data, respectively. The element a_i^j of the matrix A is defined as the path length of the ith beam inside the jth voxel, $i = 1,\ldots,I$ and $j = 1,\ldots,J$ (through enumeration of the beams is used in all projections).

As applied to flow tomography, system (2.1) has the features that it is significantly underdetermined ($I \ll J$) and sparse, i.e., the majority of the elements of the matrix A are equal to zero, and it also has large values of I and J. A number of iterative algorithms have been developed for solution of such systems. The most popular algorithm in tomography is the Algebraic Reconstruction Technique (ART). As in [7], the $(k+1)$th iterative solution for the ART is written as

$$g^{(k+1)} = g^{(k)} + \lambda^{(k)} \frac{f_{i(k)} - (a^{i(k)}, g^{(k)})}{\|a^{i(k)}\|^2} a^{i(k)}, \quad \|a^{i(k)}\| \neq 0, \quad g^{(k+1)} = g^{(k)}, \quad \|a^{i(k)}\| = 0, \tag{2.2}$$

where $a^{i(k)}$ is the $i(k)$th row of the matrix A, $\lambda^{(k)}$ is the relaxation parameter, and $i(k) = [k(\mathrm{mod}\, I) + 1]$, i.e., the rows of the matrix A are exhausted in a cycle. The scalar product and the norm in R^J are defined in the usual way. Herman [7] noted that the iterative process (2.2) converges if $0 < \lambda \leqslant 2$ for any first guess $g^{(0)} \in \mathrm{R}^J$. The ART is used in the present work for solution of the model problem in the absence of an opaque body.

The use of algorithm (2.2) for flow reconstruction in the presence of an opaque body leads to severe distortions. These distortions occur because the projection values at the points shaded by the opaque body vanish, whereas, strictly speaking, the integrals of the function $g(x, y, z)$ that are taken along the corresponding straight lines crossing the opaque body do not vanish. Thus, some equations of system (2.1) become inadequate for the problem, but algorithm (2.2) ignores this circumstance.

In this case, the natural method of correcting the result is to omit equations that became inadequate and to solve the resultant system by the ART. In the present work, this approach was implemented as follows. We call the projection taking two values, namely, 0 (the corresponding beam does not cross the body) and 1 (otherwise), a *shadow of the body.* It was assumed that the shadows from the opaque body are known in the same directions as the projection of the function to be reconstructed, both being specified on identical grids. The following algorithm was used instead of (2.2):

$$g^{(k+1)} = g^{(k)} + \lambda^{(k)} \frac{f_{i(k)} - (a^{i(k)}, g^{(k)})}{\|a^{i(k)}\|^2} a^{i(k)}, \quad \|a^{i(k)}\| \neq 0,$$

$$g^{(k+1)} = g^{(k)}, \quad \|a^{i(k)}\| = 0, \quad g^{(k+1)} = g^{(k)}, \quad f^{\mathrm{op}}_{i(k)} = 1.$$

Here $f^{\mathrm{op}} \in \mathrm{R}^I$ is the vector corresponding to the shadows from the opaque body, and the other notation is the same as in (2.2).

3. Numerical Simulations. General Remarks. The capabilities of the methods of three-dimensional tomography for reconstruction from data obtained in an aerophysical experiment were studied in the process of numerical simulation. The function

$$g(x, y, z) = \sum_{l=1}^{5} g_l(x, y, z), \tag{3.1}$$

where

$$g_l(x, y, z) = \begin{cases} 1 - \dfrac{r_l^2}{\rho_l^2}, & r_l^2 \leqslant \rho_l^2, \\ 0, & r_l^2 > \rho_l^2, \end{cases}$$

$$r_l = (\alpha_l((x - x_l)^2 + (y - y_l)^2))^{1/2} + \gamma_l z; \quad z_1 \leqslant z \leqslant z_2,$$

$$x_l = p_l \cos(2\pi\omega_l(z - z_1) + \varphi_l), \quad y_l = p_l \sin(2\pi\omega_l(z - z_1) + \varphi_l),$$

was chosen as the three-dimensional model.

In addition, the function $g(x, y, z)$ is limited in amplitude by unity, i.e., if the sum in (3.1) is larger than 1, its value is replaced by unity. Each of the functions $g_l(x, y, z)$ can be represented as a paraboloid in the variables (x, y) that is specified in the region where this paraboloid takes nonnegative values, with the vertex at the point $[x_l(z), y_l(z)]$. The functions $x_l(z)$ and $y_l(z)$ determine the rotation of the paraboloid vertex about the z axis with frequency ω_l and initial phase φ_l, the distance to the rotation axis being linearly dependent on the z coordinate with the factor γ_l.

Since the objective of the numerical simulation is to study the aspects of tomographic reconstruction of a flow structure of complex form in the presence of an opaque body rather than the flow around the solid body itself, the authors did not intend to develop a model of some realistic flow. The chosen model only outlines swirled streamlines that could be formed in principle in a flow around a rotating cone by heated gas streams.

TABLE 1

l	ρ	α	p	γ	ω	φ, deg	l	ρ	α	p	γ	ω	φ, deg
1	0.15	3.0	0.7	−0.7	1.85	0	4	0.15	3.0	0.7	−0.7	2.00	216.0
2	0.15	3.0	0.7	−0.7	1.95	72.0	5	0.15	3.0	0.7	−0.7	1.90	288.0
3	0.15	3.0	0.7	−0.7	2.00	144.0							

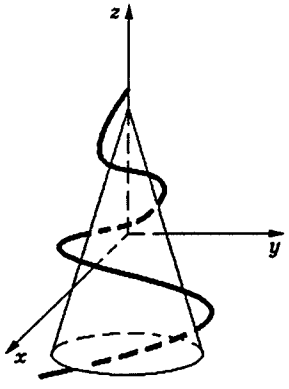

Fig. 2

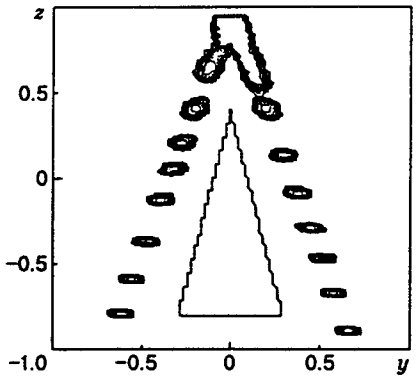

Fig. 3

In this interpretation of the model, some averaged value ω would characterize the angular rotation velocity of the cone, and the values of γ_l would be close to the tangent of the apex angle of the cone. The quantities α_l and ρ_l would determine the radius of the hot gas stream crossed by the plane $z = \text{const}$. It is assumed that the change in the refractive index because of the increase in temperature is maximum in the center of this cross section (where it is equal to 1 in conventional units) and decreases toward the periphery according to a quadratic law.

The parameters that specify five functions $g_l(x, y, z)$ are presented in Table 1.

Figure 2 shows a schematic of the cone and one of the gas streams around it. Isolines of the model in the section by the plane $x = 0$ are plotted in Fig. 3.

A cube whose center is at the coordinate origin and whose side length is equal to 2 in dimensionless units is considered as the reconstruction domain. As the opaque body a straight cone is chosen whose axis coincides with the z axis, the apex is located at the point $(0, 0, 0.4)$, its height is 1.2, and the radius of its base is 0.3.

In modeling projection data, six projections were calculated in directions perpendicular to the z axis, and the angles with the positive direction of the x axis were 80, 100, 180, 190, 340, and 350°. This distribution of projections over the angles reflects the specific features of data acquisition in flow diagnostics. As a rule, the flow examined in experiments is surrounded by the nontransparent wall of a wind tunnel, which has a limited number of windows for flow observation. It is possible to take projections only within a narrow range of angles through each window. In our numerical experiment, we simulate data collected in a facility with three windows in the 0, 90, and 180° directions, with two projections taken in each window.

The reconstruction domain was sampled into 101 × 101 × 101 voxels. 129 × 129 grids were specified on the projections' supports. To estimate numerically the quality of the reconstruction, we used the normalized root-mean-square error

$$\Delta = \left(\sum_{j=1}^{J} (g_j^{\mathrm{m}} - g_j^{(k)})^2 \Big/ \sum_{j=1}^{J} (g_j^{\mathrm{m}})^2 \right)^{1/2}, \tag{3.2}$$

where g_j^{m} and $g_j^{(k)}$ are the values of the function for the jth voxels of the model and for the iterative solution,

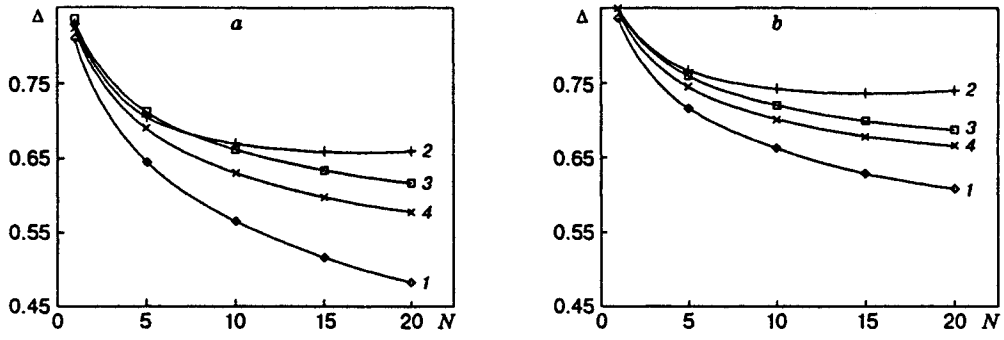

Fig. 4

respectively. [The percentage estimate of the error of the solution is obtained from (3.2) by multiplying by 100.] In describing the results, it is more convenient to change the definition of iteration for the ART used in Sec. 2. The iteration is now understood as a cycle in which all projection data are processed once. Thus, this "large" iteration corresponds to I iterations defined previously.

Reconstruction from Ideal Data. Some results of reconstruction from ideal data are represented by curves 1 in Fig. 4, which illustrates the value of Δ versus the iteration number N. Figure 4a refers to reconstruction of the function $g(x, y, z)$ without an opaque body. Figure 4b shows the reconstruction of the same function in the presence of an opaque body. It is seen from a comparison of curves 1 in Fig. 4 that an opaque body does not in principle affect the character of the convergence of the algorithm, but the value of Δ increases by approximately a factor of 1.3.

The quality of the reconstruction in the presence of an opaque body can be visually estimated in Fig. 5, which shows isolines of the reconstruction from six ideal projections in the section by the plane $x = 0$ after 20 iterations of the ART.

Reconstruction from Noisy Data. Preliminary Processing of Projections. To study the stability of the algorithm to errors in the initial data, we used the following model of random noise in projection data. The noise was assumed to be normally distributed with a zero mean and a variable dispersion, which was 30% of the projection value at the point considered. Such a high level of noise was chosen to demonstrate the effectiveness of preliminary data processing and also the advantages of adaptive frequency filtration of projections in comparison with their averaging in a moving window.

Preliminary filtration of projections is sometimes used in tomography to improve the quality of the reconstruction if there is considerable noise (see, e.g., [2–4]). In this paper, we consider two types of filtration: averaging in a moving 3×3 window and low-frequency filtration.

The filter H_Ω was used for low-frequency filtration of projections. The use of three-dimensional analogs of this filter in tomography was described in [9]. The filter H_Ω is described as follows. The value of the Fourier image of each projection at the node (ν_k, ν_l) is filtered according to the equation $H_\Omega \tilde{f}(\nu_k, \nu_l) = \tilde{f}(\nu_k, \nu_l)/[1 + \alpha(\nu_k^2 + \nu_l^2)]$. Assuming that the filter introduces distortions in projections that are similar to noise-produced distortions, the regularization parameter α was determined from the residual criterion

$$\sum_{k,l} |\tilde{f}(\nu_k, \nu_l) - H_\Omega \tilde{f}(\nu_k, \nu_l)|^2 = \delta^2 \|\tilde{f}\|^2, \tag{3.3}$$

where δ^2 is the estimate of the noise norm: $\delta^2 = \sigma^2 \Big/ \Big[\sum_{k,l} f^2(\nu_k, \nu_l)\Big]$ (σ^2 is the total dispersion of the noise).

In this paper, Eq. (3.3) was solved numerically by the halving technique.

Numerical simulations show that preliminary data processing improves the quality of the reconstruction. Frequency filtration of projections ensures the best results. This is illustrated in Fig. 4, where curves 2 correspond to the reconstruction without preliminary processing of projections and curves 3 and 4 correspond to the reconstruction obtained using smoothed and H_Ω-filtered projections, respectively.

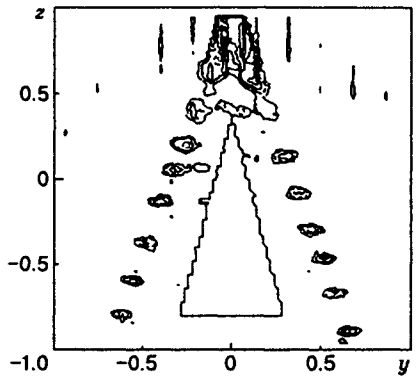

Fig. 5

Based on a theoretical analysis and a numerical simulation, we have shown that satisfactory tomographic reconstruction of complex three-dimensional flows near opaque bodies is possible. In numerical simulations, the root-mean-square error in reconstructing the model of a complex flow with vortex structures from six nonuniformly distributed projections was found to vary from 35 to 70%, depending on the presence or absence of an opaque body and noise. This result is quite satisfactory for reconstruction of such a complex three-dimensional model from such a limited set of projection data. In particular, it is seen from a comparison of Figs. 3 and 5 that the basic typical features of the density distribution are reconstructed fairly well.

In reconstruction from projections with random noise, preliminary frequency filtration of projections is the most effective method. For this purpose, we have proposed a two-dimensional low-frequency regularizing filter. The regularization parameter has been calculated from the overall norm of the noise of the projections.

This work was supported by the Russian Foundation for Fundamental Research (Grant No. 95-02-03615).

REFERENCES

1. G. N. Minerbo, J. G. Sanderson, D. B. van Hulsteyn, et al., "Three-dimensional reconstruction of the x-ray emission in laser imploded targets," *Appl. Optics*, **19**, No. 10, 1723–1728 (1980).
2. N. G. Preobrazhenskii and V. V. Pikalov, *Unstable Problems of Plasma Diagnostics* [in Russian], Nauka, Novosibirsk (1982).
3. A. L. Balandin, A. V. Likhachov, V. N. Panferov, et al., "Emission microtomography of plasma," *Proc. SPIE*, **1843**, 68–82 (1992).
4. V. V. Pikalov and N. G. Preobrazhenskii, *Reconstructive Tomography in Gas Dynamics and Plasma Physics* [in Russian], Nauka, Novosibirsk (1987).
5. C. M. Vest, *Holographic Interferometry*, Wiley, New York (1979).
6. D. Vukičević, H. Jäger, T. Niger, et al., "Tomographic reconstruction of the temperature distribution in a convective heat flow using multidirectional holographic interferometry," *Appl. Optics*, **28**, No. 8, 1508–1516 (1989).
7. G. T. Herman, *Image Reconstruction from Projections: The Fundamentals of Computerized Tomography*, Academic Press, New York (1980).
8. A. V. Likhachov and V. V. Pickalov, "A modification of the ART method for cone-beam tomography of high spatial resolution," in: *Computerized Tomography*: Proc. Fourth Int. Symp. (Novosibirsk, Russia, 1993), VSP, Utrecht (1995), pp. 309–317.
9. A. V. Likhachev and V. V. Pikalov, "Frequency filtration in algebraic algorithms of three-dimensional tomography," *Avtometria*, No. 4, 83–89 (1995).